Neuropharmacology 143 (2018) 217–227

Contents lists available at ScienceDirect

Neuropharmacology

journal homepage: www.elsevier.com/locate/neuropharm

Varenicline reduces DNA damage, tau mislocalization and post surgical cognitive impairment in aged mice

Chunxia Huang[a,b,d], John Man-Tak Chu[a,b], Yan Liu[a,b], Raymond Chuen-Chung Chang[b,c,**], Gordon Tin-Chun Wong[a,*]

[a] Department of Anaesthesiology, LKS Faculty of Medicine, The University of Hong Kong, Pokfulam, Hong Kong SAR, China
[b] Laboratory of Neurodegenerative Diseases, School of Biomedical Sciences, LKS Faculty of Medicine, The University of Hong Kong, Pokfulam, Hong Kong SAR, China
[c] State Key Laboratory of Brain and Cognitive Sciences, The University of Hong Kong, Pokfulam, Hong Kong SAR, China
[d] Department of Anaesthesiology, The Second Hospital of Anhui Medical University, Hefei, China

HIGHLIGHTS

- Laparotomy leads to neuroinflammation, neuronal apoptosis & cognitive decline.
- Tau phosphorylation & mislocalization and DNA damage are also seen postoperatively.
- Elevation in proinflammatory cytokines resolves but glia activation persists.
- Varenicline attenuates these changes & improves postoperative cognitive performance.

ABSTRACT

Postoperative cognitive dysfunction (POCD) occurs more frequently in elderly patients undergoing major surgery. Age associated cholinergic imbalance may exacerbate postoperative systemic and neuroinflammation, but the effect nicotinic acetylcholine receptor (nAchR) stimulation on the development of POCD remains unclear. Aged male C57BL/6N mice (18 months old) underwent a midline laparotomy or were exposed to sevoflurane anesthesia alone (4–5%), with or without concomitant varenicline, a partial nAchR, at 1 mg/kg/day. Laparotomy increased pro-inflammatory cytokines in the liver and hippocampus (IL-1β and MCP-1) and induced a decline in cognitive performance, indicated by lower discrimination index in the Novel Object Recognition test, greater error number and longer escape latency in the Y-maze test. Glia activation, aberrant tau phosphorylation (AT8) and accumulation of phosphorylated H2AX in the hippocampus were detectable up to postoperative day 14, with neuronal apoptosis seen in the hippocampus. Perioperative varenicline attenuated the cognitive decline and associated tau protein mislocalization, DNA damage and neuronal apoptosis. The modulation of JAK2/STAT3 signaling may play a critical role in this process. Neuroinflammation, tau phosphorylation and DNA damage contribute to the development of cognitive dysfunction following laparotomy. Cholinergic stimulation by varenicline attenuated these changes through preventing the mislocalization of phosphorylated tau and DNA damage.

1. Introduction

The number of patients that would be affected by postoperative cognitive dysfunction (POCD) is likely to increase as a result of enhanced longevity and increased number of surgical procedures being performed on patients in this age group. Perceived dysfunction in memory, attention, action and perception can impact on activities of daily living (Schwarz et al., 2013). In the longer term, POCD is associated with higher mortality, longer hospitalization and greater risk of social costs (Steinmetz et al., 2013; Tuman et al., 1992). It is recognized that advanced age, early POCD or major postoperative infection are significant risk factors for longer-term cognitive dysfunction (Abildstrom et al., 2000; Tuman et al., 1992). Structural and biochemical variations in the hippocampus accompanying normal aging may contribute to the development of cognitive impairment (Driscoll et al., 2003).

Many pathological processes underlying POCD remain unclear. Acute or chronic defective DNA repair has been linked with neurodegenerative disorders such as Alzheimer's or Parkinson's diseases (Adamec et al., 1999); (Bender et al., 2006). The consequences of DNA double-strand breaks (DSBs) include cell cycle arrest and cell apoptosis. Whether these changes occur in the brains of patients afflicted with POCD is not known. In the aging brain, there is a widespread decline in the numbers of nicotinic acetylcholine receptors (nAChRs), associated

* Corresponding author. Department of Anaesthesiology, The University of Hong Kong, Room K424, Queen Mary Hospital, Pokfulam, Hong Kong.
** Corresponding author. School of Biomedical Sciences, University of Hong Kong, L4-49, Laboratory Block, 21 Sassoon Road, Hong Kong.
E-mail addresses: rccchang@hku.hk (R.C.-C. Chang), gordon@hku.hk (G.T.-C. Wong).

https://doi.org/10.1016/j.neuropharm.2018.09.044
Received 28 December 2017; Received in revised form 2 September 2018; Accepted 26 September 2018
Available online 28 September 2018

with progressive cognitive impairment. These receptors are also required for the function of the inflammatory reflex that attenuates inflammation-mediated injuries (Rosas-Ballina et al., 2011). Consequently, subunits of nAChRs in the central nervous system have been regarded as potential therapeutic targets for neurodegenerative and psychiatric diseases (Picciotto et al., 2002; Posadas et al., 2013; Terrando et al., 2015). Varenicline (Chantix™) as a partial agonist selective for α4β2-nAChR subtypes and was approved by the FDA for smoking cessation in 2006. Acute administration of varenicline can prevent memory impairment (Kruk-Slomka et al., 2012) or enhance working and declarative memory in animals and healthy adults (Gould et al., 2013); (Mocking et al., 2013). In contrast, long-term treatment with varenicline failed to have any impact on cognition in those with established Alzheimer's disease (Kim et al., 2014). However, any potential beneficial effect of this drug on the brain following acute surgical trauma has not been investigated.

Given that there are similarities in clinical manifestations between POCD and Alzheimer's disease, we hypothesized that DNA damage occurs postoperatively in the brains of aged animals and such changes may be minimized by varenicline. The objective of this study is to first demonstrate the abnormal tau phosphorylation and DNA damage takes place in the brain after peripheral surgical trauma and such changes are accompanied by cognitive impairment. Thereafter, we evaluate the effect of varenicline on cognition and these pathological changes in the perioperative period.

2. Materials and methods

2.1. Animals

Eighteen-month-old male C57BL/6N mice were obtained from the Laboratory Animal Unit of The University of Hong Kong. All experimental protocols and animal handling procedures were approved by the Faculty Committee on the Use of Live Animals in Teaching and Research in The University of Hong Kong. A total of 108 mice were used in two sets of experiments. For the first set of experiments, the animals were divided into three groups: control (CON), sevoflurane anesthesia (SEVO) and laparotomy under sevoflurane anesthesia (LAP) to evaluate the inflammatory responses at 4 h following the different treatments. For the second set of experiments, the mice were randomly divided into 6 groups with normal saline (NS) or varenicline (Var) administration: CON + NS; SEVO + NS; LAP + NS; SEVO + Var; LAP + Var and Var, to characterize the effect of perioperative varenicline administration on behavioral and pathological changes at around 14 days following laparotomy (Fig. 1A).

2.2. Surgical procedure

A laparotomy was performed under sevoflurane anesthesia with minor modifications (Qiu et al., 2016). With the animal placed on the heating pad and using a rodent inhalation anesthesia apparatus (Harvard, USA), anesthesia was induced and maintained at 4–5% sevoflurane (Sevorane™, Abbott, Switzerland) with 0.8 L/min oxygen flow. A 2.5 cm longitudinal midline incision was made through the skin, abdominal muscle and the peritoneum. Approximately 10 cm of the intestine was exteriorized and vigorously rubbed for 30 s. The bowel loops were exposed outside the abdominal cavity for 1 min and then was replaced into the abdominal cavity. Sterile chromic gut sutures (4-0, PS-2; Ethicon, USA) were used to suture the peritoneal lining and abdominal muscle in two layers and the skin. During the procedure, the rhythm and frequency of respiration and the color of paw was monitored and the process was completed within 15 min. Mice from the anesthesia only group were subjected to sevoflurane anesthesia for 15 min at the same concentrations and gas flow.

2.3. Varenicline treatment

Varenicline (Champix, Pfizer, Germany) was dissolved in 0.9% normal saline. After sonication, varenicline solution (1 mg/kg/day) or equivalent volume of vehicle was administrated orally by gavage starting from one day before experimentation and continued for total 14 days. The dosage was determined from our preliminary experiments.

2.4. The open field test (OFT)

Based on rodents' innate tendencies to avoid open spaces, the OFT is a classic experimental tool to evaluate general locomotor activity and anxiety (Tovote et al., 2015). The spontaneous activity was characterized in the first 5 min in an enclosed gridded arena (40 cm × 40 cm × 40 cm) on postoperative day (POD) 11. A central area of 20 cm × 20 cm was demarcated with equal distance of 10 cm to each side of the arena. Total exploration time in the central area was calculated as the parameter for anxiety, and grid line crossing frequency was also counted as indicative of the locomotor activity.

2.5. The novel object recognition (NOR) task

To evaluate the animals' ability to recognize a novel object in a control environment (Leger et al., 2013), the NOR task was performed from POD 11 to 13. Twenty-four hours after habituation in the open-field arena in the absence of objects, the mice were placed in the arena containing two identical sample objects (A + A) for 10 min. After a retention interval of 24 h, the mice were returned to the same arena with two objects, with one is identical to the sample and the other being novel (A + B). One of the test objects was Falcon tissue culture flask (9.5 cm high × 2.5 cm deep × 5.5 cm wide) filled with blue sand, the other one was a paper box filled with sand, and wrapped with different color of waterproof tape as follows, yellow-blue-yellow-red-green-yellow-blue-yellow. The two subjects were of the same size. The discrimination index was used to evaluate the recognition memory and is the ratio of the exploration time between two objects. During both familiarization and testing phases, objects were located in opposite and symmetrical corners of the arena, and the location of novel versus familiar object were counterbalanced within each batch of experiment.

2.6. The rotarod training and test

Accelerated Rotarod test was performed to measure fore and hind limb motor coordination and balance, and repeated Rotarod test could be used to evaluate the motor function and memory (Shiotsuki et al., 2010). A Panlab apparatus in an accelerating paradigm (Roto-rod series 8, IITC Inc./Life Science, USA) was used to perform preoperative training and postoperative testing. Training task consisted 3 sets of constant speed training (4 rpm for a maximum of 180 s) followed by one set of accelerating training (4–20 rpm, maximum time of 5 min; speed increasing every 8 s) on the first day. Four trials of accelerating training were performed each day during the following two consecutive days. Testing was then applied on POD 13 by using the same accelerating training protocol. The mean latency to the animal falling off the apparatus was recorded and used in the subsequent analysis.

2.7. Y-maze active avoidance task

The Y-maze task was used to assess aversive memory, a hippocampal dependent place learning (Wan et al., 2007). The apparatus consisted of three plastic arms 32 cm (long) × 10 cm (wide) × 10 cm (high), and two of them are black with the floor of 3.175 mm stainless steel rods (8 mm apart), and one is white with a transparent ceiling. During the preoperative training, each mouse was allowed to freely explored the three arms for 8 min. Thereafter the animal was placed in one of the black compartments and electric shocks (2 Hz, 10 s,

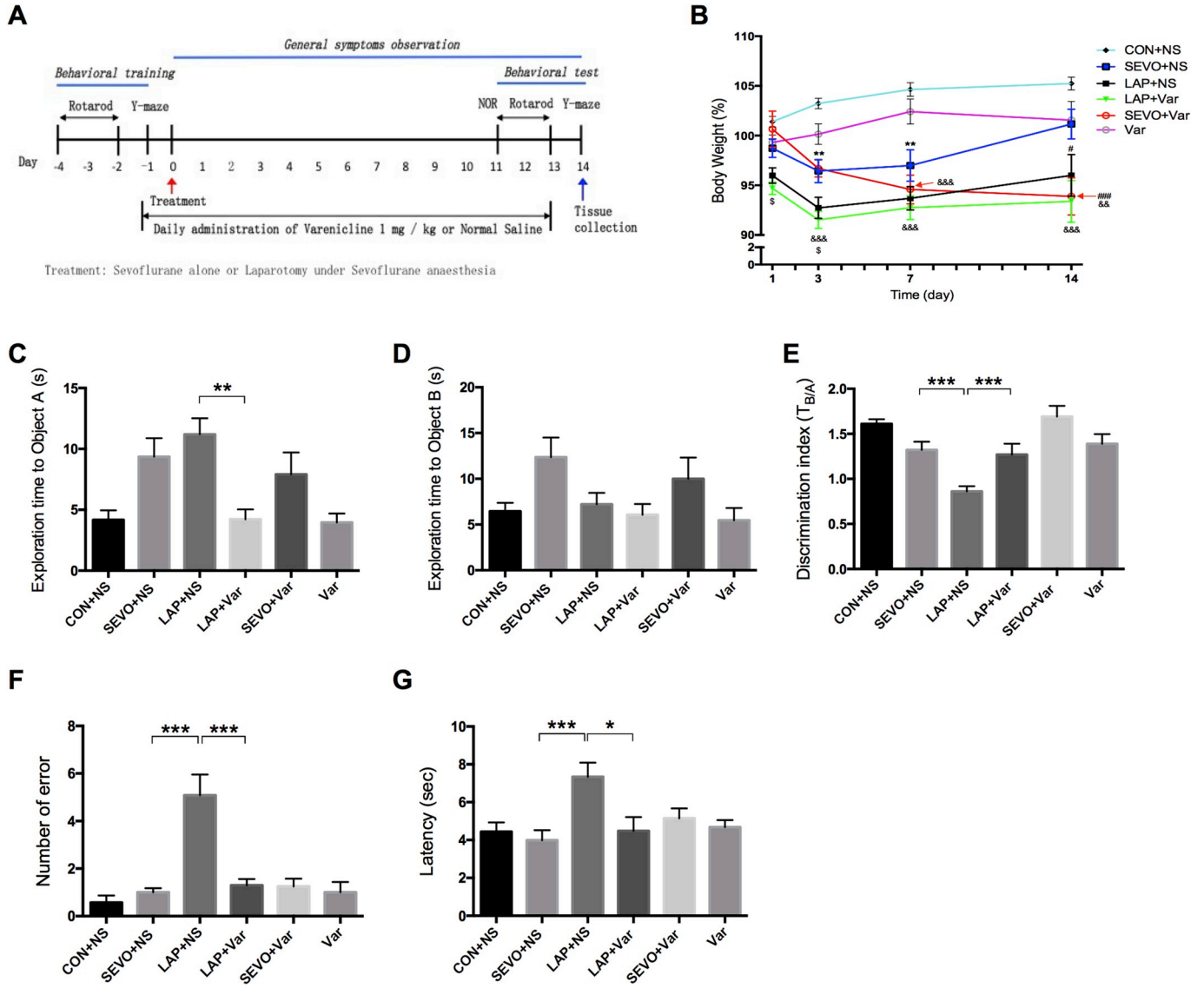

Fig. 1. Experimental workflow, bodyweight and cognitive performance following surgery. (**A**) Experimental workflow. General symptoms observations included body weight and rectal temperature during the postoperative period. The behavioral tests consisted of Novel Object Recognition (NOR) test from postoperative day (POD) 11–13, Rotarod test on POD 13 and Y-maze test on POD 14. (**B**) Body weight as a percentage of baseline were evaluated on PODs 1, 3, 7 & 14 and analyzed using a two-way ANOVA analysis with Tukey's *post hoc* test, F = 2.157, $P = 0.0077$. POD 1, $^{\$}P = 0.0135$ *vs.* SEVO + Var; on POD 3, $^{**}P = 0.0057$ *vs.* CON + NS, $^{\$}P = 0.0492$ *vs.* SEVO + Var, $^{\&\&\&}P = 0.0001$ *vs.* Var; on POD 7, $^{**}P = 0.0011$ *vs.* CON + NS, $^{\&\&\&}P = 0.0007–0.0001$ *vs.* Var; on POD 14, $^{\#}P = 0.0495$, $^{\#\#\#}P = 0.0009$ *vs.* SEVO + NS, $^{\&\&\&}P = 0.0004$, $^{\&\&}P = 0.0011$ *vs.* Var. (**C-D**) Exploration time to the objects A and B for the NOR test. (**E**) Discrimination index (DI) for the NOR test on POD 13. The DI is the ratio of the exploration time with the new object B to the old object A ($^{*}P = 0.0124$, $^{***}P < 0.0001$). To assess if there was the object preference, DI was also assessed during the familiarization session as the ratio of exploration time with two similar objects ($T_{A/A}$). Similar DI was observed between groups (data not shown). (**F-G**) The number of errors made and the escape latency for the Y-maze test on POD 14 ($^{*}P = 0.0328$, $^{***}P = < 0.0001$). CON + NS and Var (n = 12), SEVO + NS, LAP + NS, LAP + Var, SEVO + Var (n = 15). Data present as mean ± SEM.

40 ± 5 V) were applied until the animal enters the shock-free compartment within 10 s and stayed there for 30 s. This was recorded as a correct choice. Successful training was defined when mice made 9 correct choices continuously with random entrance to the black compartments. For the postoperative testing on POD 14, each mouse was tested 10 times following the same procedures as in the training trial. The numbers of incorrect choices and the time taken to enter the shock-free compartment were recorded.

2.8. Brain protein and liver tissue extraction

The mice were sacrificed by CO_2 asphyxiation in accordance with the guidelines of the American Veterinary Medical Association. After transcardial blood collection for plasma preparation and perfusion, the hippocampal tissues were dissected from one hemisphere for protein extracts immediately. Whole protein lysates were prepared by mechanical homogenization in RIPA buffer containing protease and phosphatase inhibitors (Roche, Germany) on ice. Nuclear and cytoplasmic fractions were made using NE-PER Nuclear and Cytoplasmic Extraction Reagent (Thermo Fisher Scientific, USA). The other hemisphere was immediately fixed with cold 4% paraformaldehyde for further immunofluorescence staining. The liver was also removed for liver tissue analyses.

2.9. Cytokine analysis

Protein levels of IL-1β, IL-6, MIP-2, TNF-α, MCP-1 and IL-10 in whole protein lysates or plasma were determined using a customized

Milliplex Mouse Cytokine Immunoassay Kits (Millipore, USA) with Analyzer 3.1 Luminex 200 machine and analyzed on corresponding software according to the manufacturer's instructions (n = 6–8).

2.10. SDS-PAGE and western blot analysis

The hippocampal tissue was subjected to western blot analysis as described previously (n = 8). Total lysates or cellular compartment fractions were subjected to 10% or 12% polyacrylamide gels electrophoresis and transferred onto PVDF membranes. Non-specific binding sites were blocked with 5% non-fat dry milk for 1 h. Then the membranes were incubated overnight at 4 °C with specific primary antibodies. After the incubation with horseradish peroxidase-conjugated secondary antibodies (DAKO, Denmark) for 2 h, the immunoreactive band signal intensity was subsequently visualized by chemiluminescence (WesternBright™ ECL, or WesternBright™ Quantum) (Advansta, USA). All immunoblots were normalized for gel loading with β-actin or GAPDH antibodies (Sigma-Aldrich, USA). The intensities of chemiluminescent bands were measured by Image-J software (National Institutes of Health, USA).

Primary antibodies used as follows: Bax, cleaved caspase 3, Jak2, phospho-Jak2 ($Tyr^{1007/1008}$), STAT3, phospho-STAT3 (Tyr^{705}), p53, acetyl-p53 (Lys^{379}), phospho-Histone H2A.X (Ser^{139}) and Histone H2A.X were all purchased from Cell Signaling Technology. AT8 (Ser^{202}/Thr^{205}, Thermo Fisher Scientific, USA) and Cyclin D1 (Santa Cruz Biotech, USA) were also used.

2.11. RNA isolation and real time PCR

Under RNase-free conditions, the brain and liver tissue were separately homogenized using Tri Reagent® (MRC, USA). RNA quality was assessed by optical density (OD) measurement (Nanodrop1000; Thermo Fisher Scientific, USA) as well as gel electrophoresis (1% (w/v) agarose). Only isolated RNA samples with an OD260/280 ratio > 1.8 and OD260/230 ratio < 2.0 were used for analysis (n = 8). Isolated RNA was further purified by removing genomic DNA with an Ambion® DNA-free™ DNA Removal Kit (Invitrogen, USA), then reverse transcribed using PrimeScript™ Master Mix Kit (TAKARA, Japan). PCR was performed using StepOnePlus™ Real-Time PCR system (Applied Biosystems, USA) with the SYBR® Premix Ex Taq™ II Kit (TAKARA, Japan). The amplification conditions were 95 °C for 20 s, followed by 40 cycles of denaturation at 95 °C (15 s), extension at different gene specific annealing temperature was described in Table 1, and data capture at 72 °C (30 s). The relative levels of cytokines were normalized to those of the endogenous reference glyceraldehye-3-phosphate dehydrogenase (GAPDH) following the $2^{-\Delta\Delta Ct}$ method.

Table 1
PCR conditions for inflammatory cytokines.

Gene	Primer Sequences (5'- > 3')	Annealing temperature (°C)
Interleukin-1β (IL-1β)	F: CCTCCTTGCCTCTGATGG R: AGTGCTGCCTAATGTCCC	60
Tumour necrosis factor (TNF-α)	F: CCCCAGTCTGTATCCTTCT R: ACTGTCCCAGCATCTTGT	59
Interleukin-6 (IL-6)	F: GGCAATTCTGATTGTATG R: CTCTGGCTTTGTCTTTCT	56
Interleukin-8 (IL-8)	F: TGCCGTGACCTCAAGATGTGCC R: CATCCACAAGCGTGCTGTAGGTG	60
Interleukin-10 (IL-10)	F: CCAAGCCTTATCGGAAATGA R: TTCTCACCCAGGGAATTCAA	60
Monocyte Chemoattractant Protein-1 (MCP-1)	F: TGCTGTCTCAGCCAGATGCAGTTA R: TACAGCTTCTTTGGGACACCTGCT	60
Glyceraldehye-3-phosphate dehydrogenase (GAPDH)	F: ATTCAACGGCACAGTCAA R: CTCGCTCCTGGAAGATGG	56

2.12. Immunofluorescence staining

The brain tissue was fixed for 72 h, then 6-μm-thick coronal sections from paraffin blocks, or 25-μm-thick frozen sections (from −1.46 mm to −2.46 mm posterior to the bregma) were made (n = 8). After the antigen retrieval with 0.01 M citrate buffer (pH 6.0) at 90 °C for 15 min, 10% normal goat serum was used for blocking non-specific binding. Then specific primary antibodies were applied at 4 °C overnight as follows: Iba1 (Wako, Japan), gilial fibrillar acdic protein (GFAP) (Sigma-Aldrich, USA), CD68 (Serotec, USA), AT8, γH2AX, NeuN (Chemicon, USA), pY-STAT3. Sections were then incubated with specific Alexa Fluor 568 or 488 secondary antibodies (Invitrogen, USA) for 2 h at room temperature. The counterstaining was performed with 3 μM 4′-6-diamidino-2-phenylindole (DAPI) (Sigma-Aldrich, USA). Immunolabeled tissues were observed under a laser scanning confocal fluorescent microscope (5 × , 20 × , 40 × oil and 63 × oil immersion objectives) (Carl Zeiss LSM 700, Germany) equipped with ZEN light software at 1024 × 1024 resolution. *Z*-stack images were acquired. All quantitative analyses were performed on at least four images acquired from at least four serial sections per animal from at least three independent experiments.

2.13. Apoptosis assay

Apoptosis was detected using the TdT-mediated dUTP nick-end labeling (TUNEL) technique (In Situ Cell Death Detection Kit TMR red, Roche, USA), which labels the cut ends of DNA fragments in the nuclei of apoptotic cells. The nuclei of all cells were stained with DAPI (n = 8).

2.14. Statistical analyses

The data of animal body weights were analyzed by two-Way analysis of variance (ANOVA) for repeated measures followed by the Tukey *post hoc* test, using the statistic software GraphPad Prism 6.0 (Graph Pad Software Inc., USA). Other data, such as relative mRNA levels of cytokines, normalized band intensities in western blot, quantification of immunoreactivity and quantification of $TUNEL^+$ cells, and behavioral tests were analyzed by one-way ANOVA followed by the Tukey *post hoc* test. Normality of the data and homogeneity of group variances were assessed using the D'Agostino-Pearson omnibus normality test, Shapiro-Wilk normality test and Kolmogorov-Smirnov test, respectively. Statistical significance was determined if $^*P < 0.05$. Data are represented as the mean ± SEM.

3. Results

3.1. Laparotomy induced cognitive impairment

The body weight changes during the postoperative period are shown in Fig. 1B. There was a significant body weight decline in the sevoflurane anesthetized mice (on POD 3: 96.4 ± 1.2% of baseline, $P = 0.0057$; POD 7: 97.0 ± 1.6% of baseline, $P = 0.0011$; n = 12 or 15). The decline was greater in those animals that underwent surgery compared with those exposed to anesthesia alone (92.7 ± 1.0% of baseline on POD 3, 93.7 ± 1.1% of baseline on POD 7).

Significant recognition memory impairment following surgery is seen as indicated by a lower discrimination index in the novel object recognition test (Fig. 1E, 0.86 ± 0.06, $P = 0.0124$ compared to sevoflurane anesthesia, n = 12 or 15), as well as a greater error number and longer latency in the Y-maze test (5.1 ± 0.9, $P < 0.0001$; 7.3 ± 0.7 s, $P = 0.0001$ compared to sevoflurane anesthesia, respectively; n = 12 or 15; Fig. 1F and G). Varenicline reduced these impairments without affecting the locomotor activity and motor function. The total number

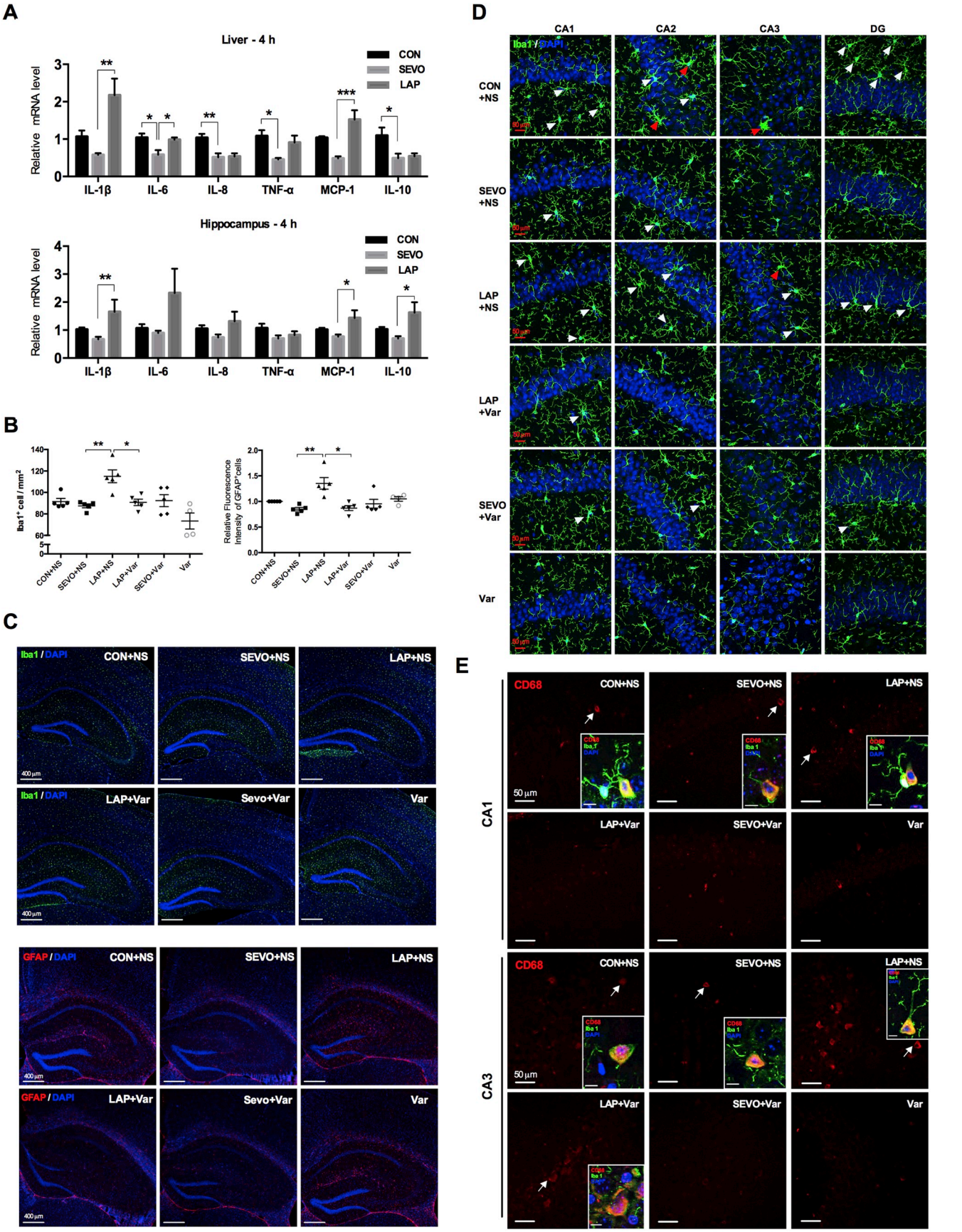

(caption on next page)

Fig. 2. Early and late inflammatory responses following by surgery. (**A**) mRNA levels for various pro- and anti-inflammatory cytokines in the liver and hippocampus at 4 h post operatively. (One-way ANOVA analysis with Tukey post hoc test for each cytokine). For the liver, IL-1β, F = 8.923; IL-6, F = 6.226; IL8, F = 9.140; TNF-α, F = 4.678; MCP-1, F = 11.89; IL-10, F = 4.980; For the hippocampus, IL-1β, F = 5.861; MCP-1, F = 4.671; IL-10, F = 4.017 ($^{*}P < 0.05$, $^{**}P < 0.01$, $^{***}P < 0.001$, n = 8). On POD 14, there was no difference in the cytokine concentrations in the either hippocampus or plasma (Supplementary Fig. S1). (**B**) Cell count of Iba1 positive microglia and immunoreactivity of GFAP-labeling astrocytes in the hippocampal coronal sections on POD 14, ($^{*}P < 0.05$, $^{**}P < 0.01$) Representative confocal photographs are shown in Supplementary Fig. S2. Data represent the mean value of 4 brain sections per mouse. For CON + NS, SEVO + NS, LAP + NS, LAP + Var and SEVO + Var (n = 5), Var (n = 4). Values in the left panel were analyzed by one-way ANOVA, F = 7.927, $^{*}P = 0.0157$, $^{**}P = 0.0045$. Values in the right panel were analyzed by Kruskal-Wallis test, Kruskal-Wallis statistic = 19.78, $^{*}P = 0.0139$, $^{**}P = 0.0030$. (**C**) Representative confocal microscopy photographs for the activation of Iba1^{+} microglia (green) and GFAP^{+} astrocyte (red) on POD 14. (**D**) Representative confocal microscopy photographs for the activation of Iba1^{+} microglia (green) in different sub regions of the hippocampus on POD 14. Following laparotomy, there were various morphological forms of microglia activation (hypertrophic, red arrow; bushy, white arrow) in the hippocampal sub-regions. (**E**) Representative photographs of cells co-expressing Iba1 and CD68 in the hippocampal CA1 and CA3 regions on POD 14 (white arrow indicating the enlarged cell in the insert). Scale bar in the small box = 4 μm. Data present as mean ± SEM.

of grid crossings and the time spent in the center field were not significantly different between the groups. Similarly the time to fall from the rotarod was not affected by either surgery or varenicline (Supplemental Fig. S2).

3.2. Early inflammatory response with a prolonged period of glial activation following surgery

Evidence for peripheral inflammation and neuroinflammation was seen at 4 h after surgery, as indicated by the increase in the mRNA levels of pro-inflammatory cytokines (Fig. 2A), such as IL-1β, IL-6 and MCP-1 in the liver (2.17 ± 0.38, $P = 0.0023$; 0.98 ± 0.06, $P = 0.0367$; 1.52 ± 0.22, $P = 0.0005$ compared to sevoflurane anesthesia, respectively; n = 8), and IL-1β and MCP-1 in the hippocampus (1.65 ± 0.34, $P = 0.0091$; 1.43 ± 0.24, $P = 0.0288$ compared to sevoflurane anesthesia, respectively; n = 8). Furthermore, surgery also induced an elevation in the mRNA level of the anti-inflammatory cytokine IL-10 in the hippocampus (1.63 ± 0.37, $P = 0.0448$ compared to sevoflurane anesthesia; n = 8). On the other hand, sevoflurane anesthesia (15 min) reduced both pro- and anti-inflammatory cytokine mRNAs (IL-6, IL-8, TNF-α, MCP-1 and IL-10) in the liver but not at the hippocampus. The concentration of cytokines in the hippocampus and in the plasma were not significantly different by POD 14 (Supplemental Fig. S1), indicating a resolution of inflammation.

The activation of Iba1^{+} microglia and GFAP^{+} astrocyte throughout the hippocampus as indicative of neuroinflammation following laparotomy was observed up to POD 14 (115.1 ± 6.0, $P = 0.0036$; 1.35 ± 0.11, $P = 0.0030$ compared to sevoflurane anesthesia, respectively; n = 4 or 5; Fig. 2B and C). Predominately activated microglia with either hypertrophic or bushy morphology were present in the hippocampus, especially in the cornu ammonis (CA) 3 and dentate gyrus (DG) regions (Fig. 2D) but perioperative varenicline attenuated this glial activation (90.8 ± 3.0, $P = 0.0118$; 0.87 ± 0.05, $P = 0.0139$ compared to laparotomy, respectively; Fig. 2B).

The co-expression of Iba1 and CD68 was also observed in CA1 and CA3 regions after laparotomy (Fig. 2E). CD68, a marker of reactive and phagocytic microglia, was up regulated in activated microglia that displayed a hypertrophic/bushy cellular morphology. This co-expression was attenuated in groups receiving varenicline, particularly in the LAP + Var group.

3.3. Laparotomy induced tau mislocalization and DNA damage

Following surgery there was a significant elevation of AT8 (Ser^{202}/Thr^{205}) in both the cytosolic and nuclear fractions of the hippocampus (2.02 ± 0.22, $P = 0.0005$; 1.56 ± 0.34, $P = 0.0027$ compared to sevoflurane anesthesia, respectively; n = 8; Fig. 3A). The presence of paired helical filament (PHF) tau in the hippocampus is a marker of disease process, possibly representing the first step in DNA damage (Morris et al., 2011). In addition, higher level of γH2AX in response to DNA double-strand breaks (Iacovoni et al., 2010) was observed in postsurgical mice (1.84 ± 0.26, $P < 0.0001$ compared to sevoflurane anesthesia). These changes were corroborated by increases in the immunoreactivity for AT8 and γH2AX. (1.50 ± 0.35, $P = 0.025$; 1.10 ± 0.07, $P = 0.0121$ compared to sevoflurane, respectively; n = 4 or 5; Fig. 3B). Perioperative varenicline attenuated both the rise in AT8 and the rise in γH2AX.

3.4. Neuronal apoptosis following laparotomy

The cellular apoptosis following surgery is indicated by large number of TUNEL^{+} cells throughout CA1 and CA3 regions (1.04 ± 0.05, $P = 0.0004$; 1.34 ± 0.14, $P = 0.0255$ compared to sevoflurane anesthesia, respectively; n = 8; Fig. 4A). The vast majority of TUNEL^{+} cells were neurons, especially in CA3 region (Fig. 4B) and the distribution of TUNEL^{+} cells in the hippocampal sub-regions are shown in Supplemental Fig. S5. Sevoflurane reduced cell death in both CA1 and CA2 regions (Fig. 4A). Perioperative administration of varenicline consistently reduced TUNEL^{+} cells following laparotomy in CA1 and CA3.

We also illustrated the significant high levels of Bax and cleaved caspase 3 in the hippocampus of postsurgical mice (2.71 ± 0.89, $P = 0.0278$; 2.11 ± 0.49, $P = 0.0021$ compared to sevoflurane, respectively; n = 8; Fig. 4C). After perioperative administration of varenicline, significant reductions of Bax and cleaved caspase 3 were observed, which was consistent with limited neuronal apoptosis shown in TUNEL staining.

3.5. Correlation of signaling pathways, DNA repair and cell cycle regulation following surgery and varenicline consumption

To investigate the effect of, if any, surgery, anesthesia and varenicline on nAChRs we measure the expression of α7-, α4-, β2-nAChRs in the hippocampus. The levels of α7 nAChR protein expression was similar but surgery reduced the levels of α4-and β2-nAChRs and this change was attenuated with varenicline administration ($P < 0.05$, Fig. 5). The increase in the expression of these subunit by varenicline alone did not reach statistical significance.

We further evaluated the signaling pathways related to the inflammation, DNA repair and cell cycle in this model. Following laparotomy, the activity of JAK2/STAT3 signaling pathway was reduced. Less STAT3 was phosphorylated at Tyr705 and translocated into the nucleus (0.63 ± 0.05, $P < 0.0001$ compared to sevoflurane anesthesia; n = 8; Fig. 6). However, sevoflurane significantly increased STAT3 phosphorylation and translocation, without affecting the activity of JAK2 through phosphorylation at Tyr1007/1008 (172 ± 17% of control, $P = 0.0073$). The limited inflammatory cytokines and TUNEL^{+} cell in the hippocampus may partially due to the enhancement of the activity of STAT3.

There were less accumulation and acetylation of p53 in the hippocampus from surgical mice, which may affect DNA repair machineries ($P < 0.0001$, $P = 0.0011$ compared to sevoflurane anesthesia, respectively). However, laparotomy affected cell cycle progression via enhancing Cyclin D1 ($P = 0.0052$ compared to sevoflurane anesthesia).

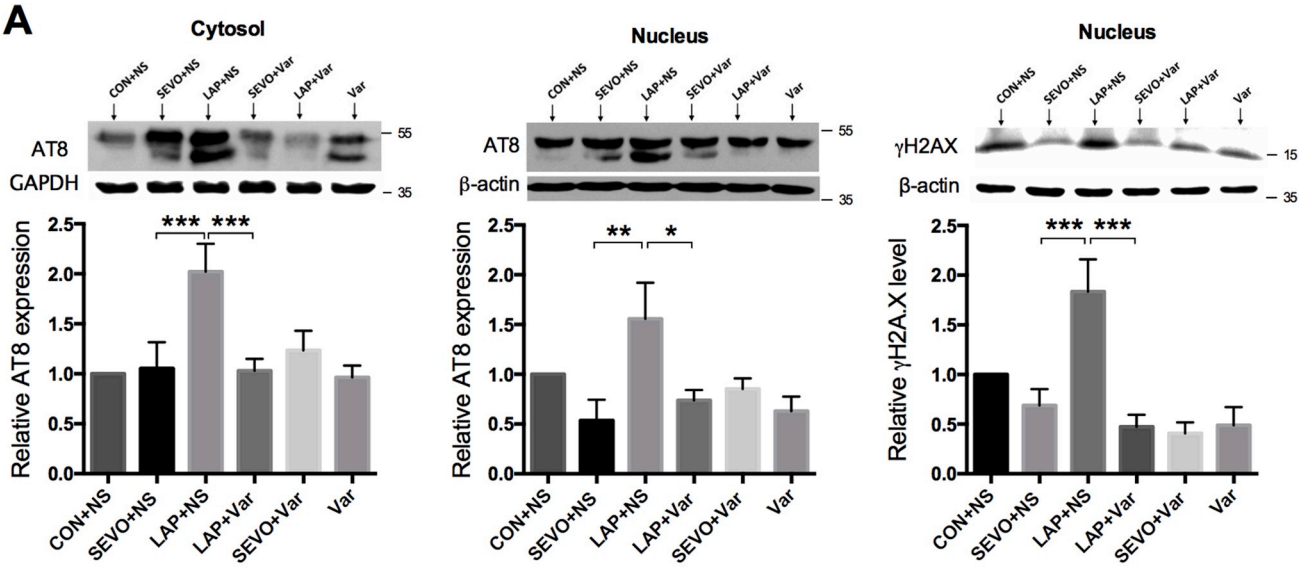

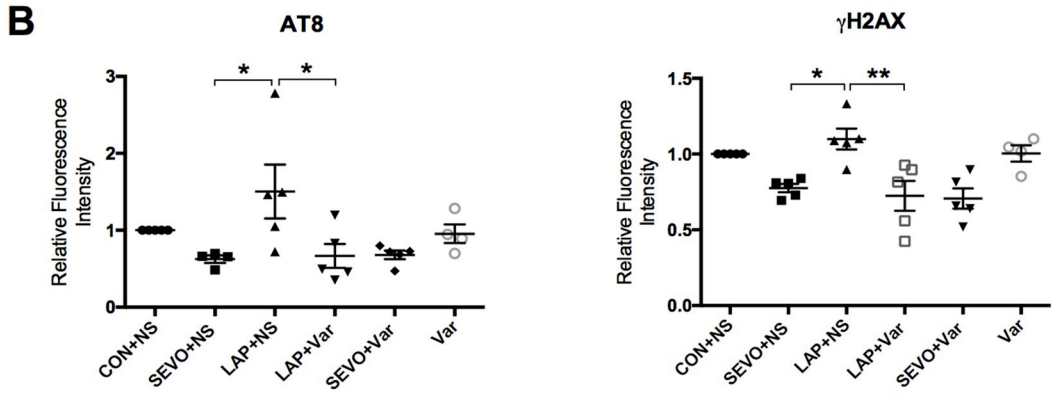

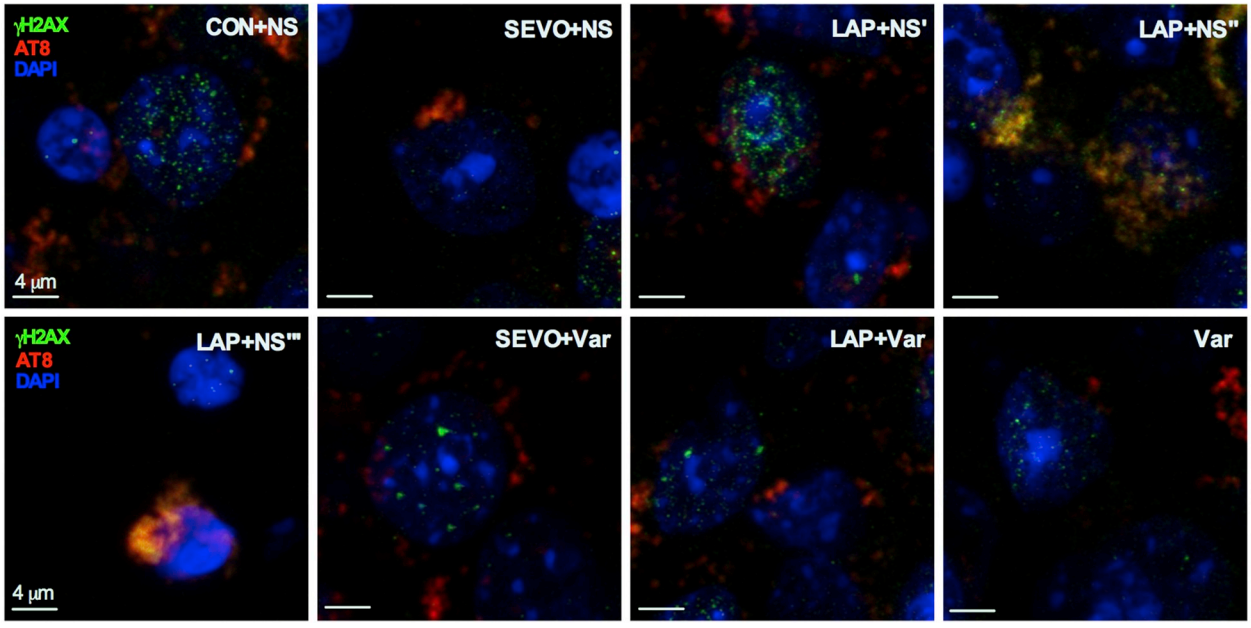

(caption on next page)

Fig. 3. Tau phosphorylation and mislocalization and DNA damage induced by laparotomy. (**A**) Relative expression of AT8 and γH2AX in the cytosolic and nuclear fractions from the hippocampus was analyzed by using one-way ANOVA (AT8 in cytosol, F = 4.481; AT8 in nucleus, F = 3.64; γH2AX, F = 9.226, $^{*}P = 0.0251$, $^{**}P = 0.0027$, $^{***}P = 0.0001–0.0005$, n = 8). AT8 was the antibody used to assess tau phosphorylation at Ser202 and Thr205. γH2AX is the phosphorylated form of histone H2AX at Ser139, occurring in response to DNA damage. (**B**) Quantitative immunoreactivity of AT8 and γH2AX in the hippocampus was analyzed by using one-way ANOVA (AT8, F = 43.712,$^{*}P = 0.0354$, $^{*}P = 0.0324$; γH2AX, F = 7.488, $^{*}P = 0.0372$, $^{**}P = 0.0037$, n = 4–5). (**C**) Photographs showing H2AX phosphorylation localized in the nucleus of the hippocampal CA3 region (*green*, CON + NS). Following laparotomy, AT8 was translocating (*red*, LAP + NS′) or translocated (*yellow*, LAP + NS″) to the nucleus and the nuclei displayed chromatin condensation (*orange*, LAP + NS‴).

Perioperative varenicline enhance the binding of p53 to DNA by promoting the acetylation at Lys379 and may facilitate DNA repair.

4. Discussion

In this study, we used an aged animal model undergoing surgery to investigate the pathological changes and a potential therapy for postoperative cognitive dysfunction. There were evidence of systemic inflammation and neuroinflammation, significant cognitive dysfunction associated with tau hyperphosphorylation and mislocalization. In addition, we were able to demonstrate the presence of DNA damage as well as neuronal apoptosis post operatively. Furthermore, perioperative varenicline administration appear attenuate the glia activation, tau mislocalization and DNA damage. The JAK/STAT pathway may play a role in mediating these events and maybe a potential mechanism underlying the effects varenicline on POCD.

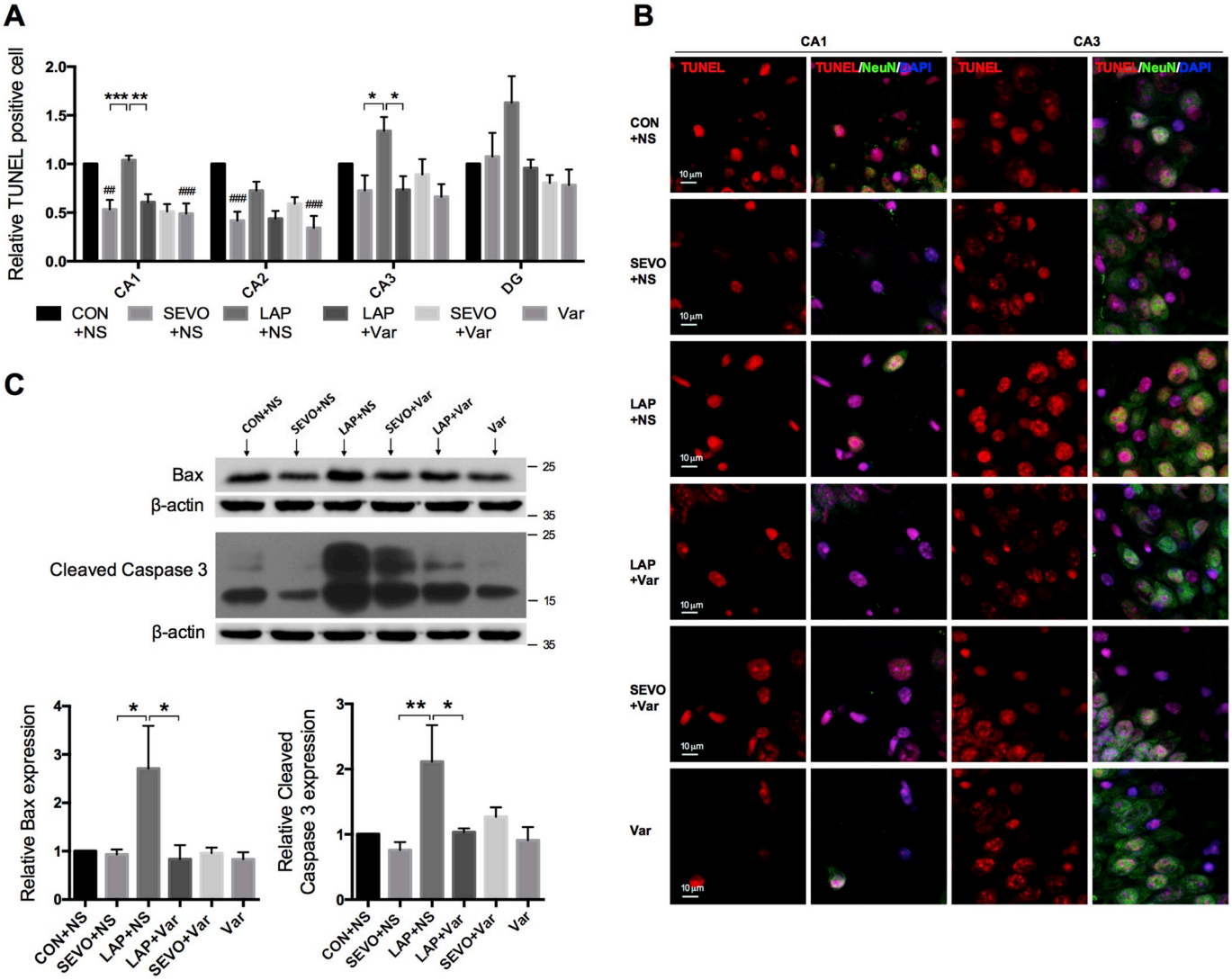

Fig. 4. Apoptosis following surgery. (**A**) TUNEL^{+} cell count in the hippocampal sub-regions (one-way ANOVA analysis with Tukey *post hoc* test, in CA1, F = 10.92, $^{**}P = 0.0034$, $^{***}P = 0.0004$; in CA3, F = 3.573, $^{*}P = 0.0255–0.0283$, n = 8). Compared to the CON + NS group, there was a significant reduction of TUNEL^{+} cells in the CA1 and CA3 regions following sevoflurane or varenicline exposure ($^{\#\#}P = 0.0013$, $^{\#\#\#}P = 0.0001–0.004$, n = 8). (**B**) Representative photographs of TUNEL^{+} cell localized in the hippocampal CA1 and CA3 regions (*red*, CON + NS). Peripheral chromatin condensation is seen in the nuclei of cells in CA1 and CA3 regions, which is a feature of caspase-dependency (*purple*). The vast majority of these cells are neurons as indicated by double labeling with the neuronal specific NeuN, especially in CA3 region (yellow). (**C**) Relative expression of Bax and Cleaved Caspase 3 in the hippocampus. The western blot analysis data was analyzed by using one-way ANOVA (F = 3.606, $^{*}P = 0.0177–0.0278$, $^{**}P = 0.0021$, n = 8). The fragmentations of cleaved caspase 3 at 17 and 19 kDa were both significantly increased following laparotomy. Data present as mean ± SEM.

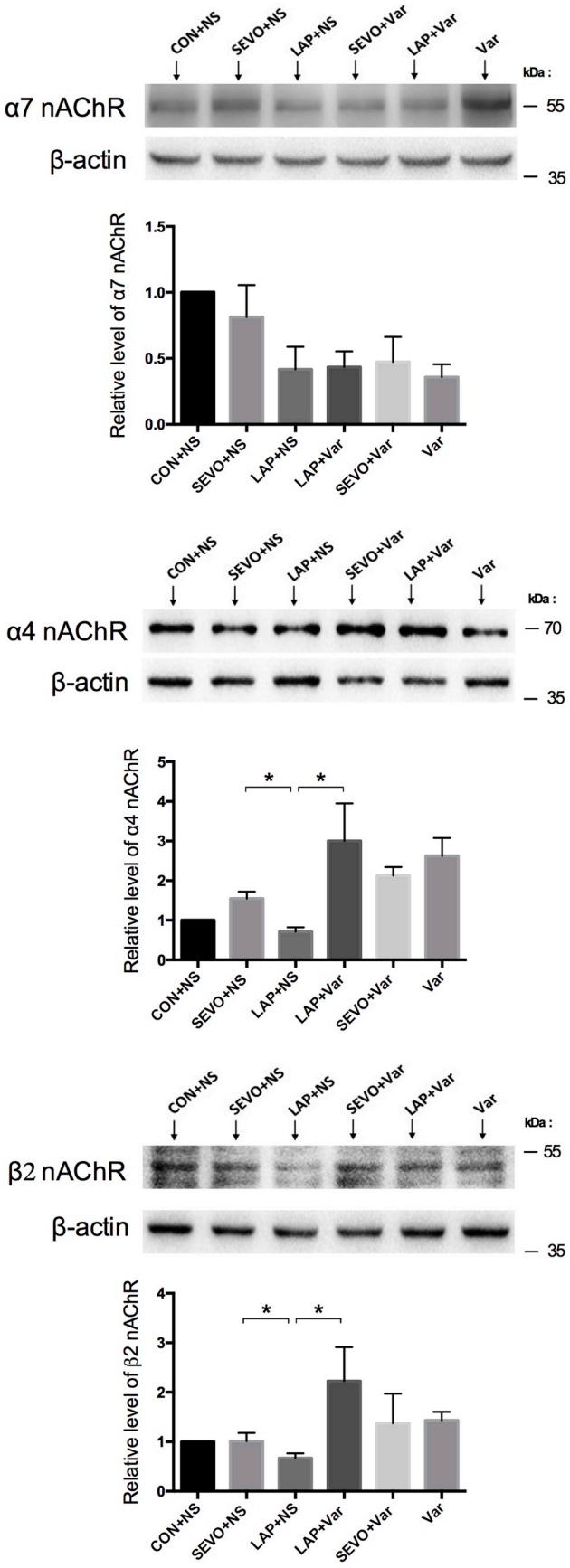

Fig. 5. The activation of nAChR after surgery with or without varenicline administration. α7-nAChRs, F = 2.742. α4-nAChRs, F = 4.104, $^{*}P$ = 0.0491, LAP + NS *vs.* SEVO + NS; $^{*}P$ = 0.0160, LAP + Var *vs.* LAP + NS. β2-nAChRs, F = 3.944, $^{*}P$ = 0.0487, LAP + NS *vs.* SEVO + NS; $^{*}P$ = 0.0183, LAP + Var *vs.* LAP + NS.

Evidence suggests inflammatory processes are involved in the early stages of neurodegenerative diseases such as Alzheimer's disease, even preceding any significant changes of Aβ and tau in the cerebrospinal fluid (CSF) of patients (Schuitemaker et al., 2009). It is not surprisingly that there was marked elevation of pro-inflammatory cytokine mRNAs both in peripherally and in the brain early in response to surgical trauma. The presence of pro-inflammatory cytokines acting on the brain could induce the prolonged cognitive impairment (Dantzer, O'Connor, Freund, Johnson and Kelley, 2008). In our current model, we could not demonstrate a sustained release of inflammatory cytokines in the brain. However we did show a persistent activation of glia in the hippocampus. Glia-mediated neuroinflammation plays a role in various tauopathies and as suggested by our data, possibly in POCD (Kamer et al., 2012; Qiu et al., 2016). Perioperative varenicline attenuated this glial activation, along with improvements in working and declarative memory. The reduction in neuroinflammation by cholinergic stimulation may be the major mediator in attenuating the development of cognitive impairment (Guzman-Mejia et al., 2018; Tyagi et al., 2010).

As microtubule-associated proteins, tau proteins stabilize microtubules as well as participate in other cellular functions such as microtubules assembly, axonal transport, neuronal polarization, axonogenesis, signal transduction and cell cycle under physiological conditions, which are controlled by phosphorylation of tau (Ittner and Gotz, 2011; Mandelkow et al., 1996; Morris et al., 2011; Tolnay and Probst, 1999; Wang and Liu, 2008). A number of neurodegenerative disorders present with prominent tau pathology in the CNS (Nilson et al., 2017). In tauopathies, the intracellular soluble tau forms filamentous structures of aggregated, hyperphosphorylated tau, which are associated with synaptic loss and neuronal death. As a hallmark finding for many neurodegenerative disorders, abnormal tau phosphorylation following laparotomy in this model may represent a major contributor to the observed cognitive impairment (Wan et al., 2010). A growing body of evidence suggests that abnormal hyperphosphorylation of tau protein may play an important role in the pathogenesis of cognitive impairment and neuronal apoptosis induced by anesthesia (Le Freche et al., 2012) or peripheral surgery (Huang et al., 2018; Li et al., 2016). The therapeutic effect of varenicline further confirmed a role of abnormal tau phosphorylation in POCD. However it is difficult to differentiate the effects of anesthesia and surgery on cognition as surgery is rarely performed without anesthesia. Clinically cognitive impairment still occurs even in postoperative patients who received regional rather than general anesthesia(Silbert et al., 2014). This type of experimental conditions would be technically challenging to reproduce using animal models.

p53 is a protein activated in response to a wide variety of stresses that can damage the DNA (Vogelstein et al., 2000). As a tumour suppressor gene, dysfunction of p53 contributes to different inflammatory diseases (Lane and Crawford, 1979); (Jackson and Bartek, 2009) possibly by regulating microglial behavior (Jayadev et al., 2011). It is therefore conceivable that the inactivation of p53 or p53 acetylation following laparotomy may contribute to the activation of microglia. In aged brains, lower levels of p53 may render them less able to activate the DNA repair processes. This may account for our findings of mild activation of microglia, higher levels of the immunoreactivity of γH2AX in the nucleus and TUNEL^{+} cells following surgery. In addition to gamma or UV irradiation, any endogenous or exogenous stimuli could cause DNA damage. In consequence to the inflammation induced by laparotomy, γH2AX predominantly expressed in the hippocampal neuronal nucleus. Inflammation maybe linked to defective DNA repair

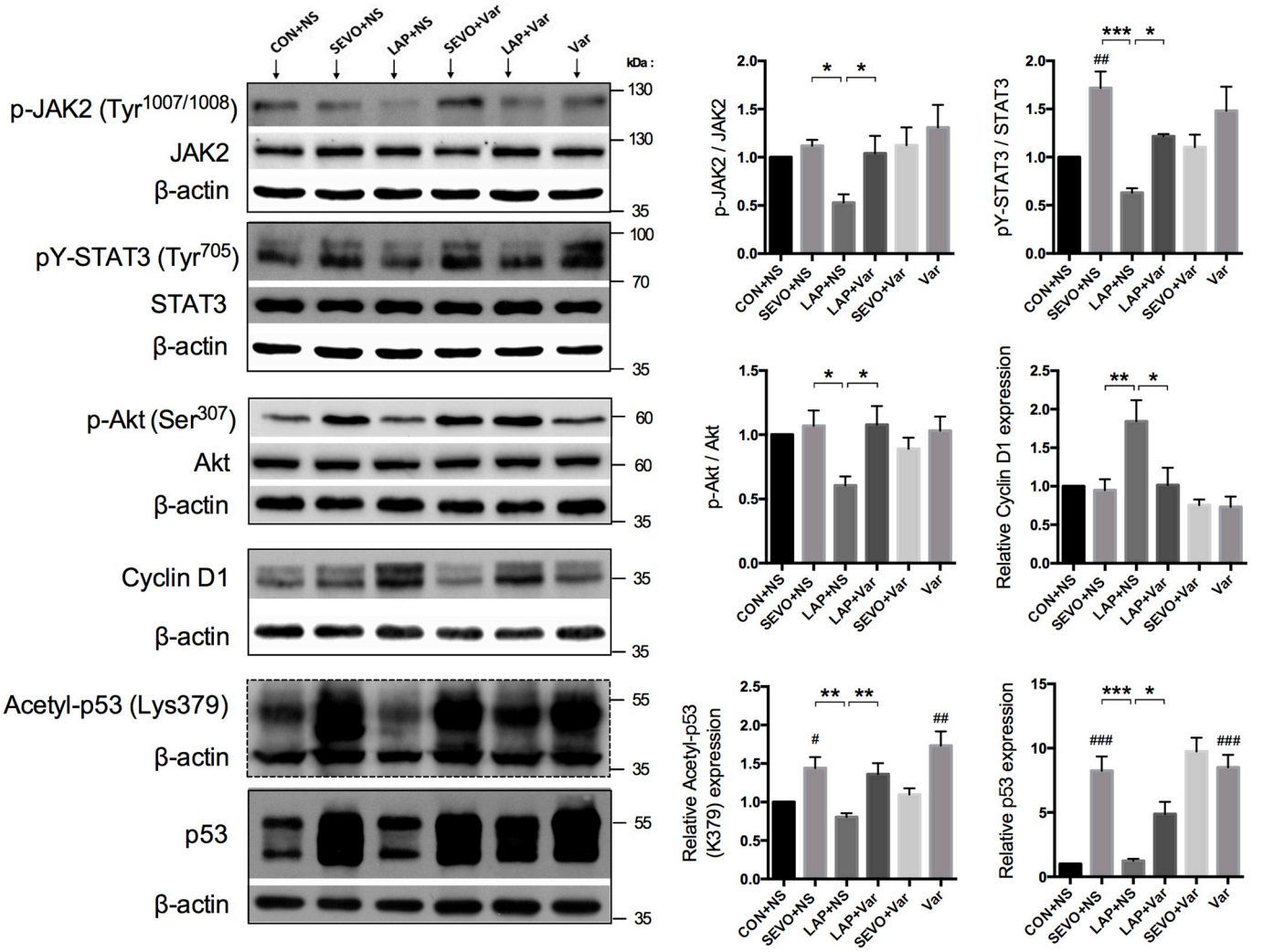

Fig. 6. Western blot analysis of the JAK2/STAT3 pathway, p53 and cell cycle regulation by Cyclin D1. Phosphorylation and translocation of STAT3 at Tyr705 was detected in the nuclear fractions ($^{\#}P < 0.05$, $^{\#\#}P < 0.01$, $^{\#\#\#}P < 0.001$ *vs.* CON + NS, n = 8). ($^{*}P < 0.05$, $^{**}P < 0.01$, $^{***}P < 0.001$, n = 8). p53, acetylated p53 and Cyclin D1 were detected in the whole protein lysates. Data present as mean ± SEM., and was analyzed by using one-way ANOVA, p-JAK2/JAK2, F = 2.459; p-YSTAT3/STAT3, F = 5.091; p-Akt/Akt, F = 3.259; Acetyl-p53, F = 7.985; p53, F = 20.66.

process resulting in cell cycle arrest and apoptosis (Hoeijmakers, 2009) and may contribute to cognitive impairment. In addition to attenuating glia activation and tau mislocalization, varenicline administration also reduced neuronal DNA damage and apoptosis and this may be linked to the increased activity of pY-STAT3, p53 and p53 acetylation in the hippocampus.

Among its involvement in multiple biological processes, the Janus-associated kinase (JAK)–signal transducer and activator of transcription (STAT3) pathway is its critical role in modulating memory (Copf, Goguel, Lampin-Saint-Amaux, Scaplehorn and Preat, 2011) and promoting cognitive flexibility (Donegan et al., 2014). This involves either the modulation of microtubule stability (Ng et al., 2006) or the regulation of synaptic plasticity (Nicolas et al., 2012). Pathological Aβ could inactivate JAK2/STAT3 contributing to the spatial working memory deficits (Chiba et al., 2009). We firstly reported that following laparotomy, the cognitive dysfunction associated with pathological tau phosphorylation and mislocalization may due to the suppression of JAK2/STAT3. The major mechanisms are the down-regulation of choline acetyltransferases (ChAT) and desensitization of M1-type muscarinic acetylcholine receptor (Chiba et al., 2009; Park et al., 2013). Cyclin D1 is a crucial cell cycle regulatory protein, and it is also part of a feed back network down-regulating STAT3 activity. Overexpression of cyclin D1 inhibits transcriptional activity of STAT3 (Bienvenu et al., 2001), which may contribute to the neuronal apoptosis, and further to the cognitive dysfunction induced by laparotomy in aged animals. However, these changes were attenuated by varenicline administration. The activation of JAK2/STAT3 induced by perioperative intervention of varenicline may raise an explanation.

One of the major limitations of this study was the lack of interrogation of cholinergic receptor system following laparotomy and varenicline administration. In addition to stimulate specific nAChRs subunits (α4β2), varenicline still could elicit the enhancement on the expression of α3β4-and α7-nAChRs (Marks et al., 2015). In our study, α7-nAChRs was not affected by laparotomy nor varenicline. Further experiments are required to more precisely determine by which mechanisms accumulated abnormal tau phosphorylation and DNA damage affect neuronal function.

In conclusion, surgery trauma in the form of a laparotomy results in cognitive impairment that is associated with neuroinflammation, tau mislocalization, DNA damage and neuronal apoptosis that may involve the JAK/STAT signaling pathway. Perioperative varenicline attenuates these changes and improves working and declarative memory impairment without affecting motor function.

Conflicts of interest

The authors have no actual or potential conflicts of interest.

Acknowledgments

This study was supported by: Seed Funding Programme for Basic Research, Hong Kong University (HKU) grant number 201311159069 and 201311159171 to GTCW; Seed Funding Programme for Basic Research (HKU) grant number 201611159183 to RCCC and General Research Fund of the University Grants Committee, Hong Kong, grant number 17123217, to RCCC, HKU Alzheimer's Disease Research Network under Strategic Research Theme on Ageing, and generous donation from Ms. Kit Wan Chow.

Appendix A. Supplementary data

Supplementary data to this article can be found online at https://doi.org/10.1016/j.neuropharm.2018.09.044.

References

Abildstrom, H., Rasmussen, L.S., Rentowl, P., Hanning, C.D., Rasmussen, H., Kristensen, P.A., Moller, J.T., 2000. Cognitive dysfunction 1-2 years after non-cardiac surgery in the elderly. ISPOCD group. International Study of Post-Operative Cognitive Dysfunction. Acta Anaesthesiol. Scand. 44, 1246–1251.

Adamec, E., Vonsattel, J.P., Nixon, R.A., 1999. DNA strand breaks in Alzheimer's disease. Brain Res. 849, 67–77.

Bender, A., Krishnan, K.J., Morris, C.M., Taylor, G.A., Reeve, A.K., Perry, R.H., Jaros, E., Hersheson, J.S., Betts, J., Klopstock, T., Taylor, R.W., Turnbull, D.M., 2006. High levels of mitochondrial DNA deletions in substantia nigra neurons in aging and Parkinson disease. Nat. Genet. 38, 515–517.

Bienvenu, F., Gascan, H., Coqueret, O., 2001. Cyclin D1 represses STAT3 activation through a Cdk4-independent mechanism. J. Biol. Chem. 276, 16840–16847.

Chiba, T., Yamada, M., Sasabe, J., Terashita, K., Shimoda, M., Matsuoka, M., Aiso, S., 2009. Amyloid-beta causes memory impairment by disturbing the JAK2/STAT3 axis in hippocampal neurons. Mol. Psychiatr. 14, 206–222.

Copf, T., Goguel, V., Lampin-Saint-Amaux, A., Scaplehorn, N., Preat, T., 2011. Cytokine signaling through the JAK/STAT pathway is required for long-term memory in Drosophila. Proc. Natl. Acad. Sci. U. S. A. 108, 8059–8064.

Dantzer, R., O'Connor, J.C., Freund, G.G., Johnson, R.W., Kelley, K.W., 2008. From inflammation to sickness and depression: when the immune system subjugates the brain. Nat. Rev. Neurosci. 9, 46–56.

Donegan, J.J., Girotti, M., Weinberg, M.S., Morilak, D.A., 2014. A novel role for brain interleukin-6: facilitation of cognitive flexibility in rat orbitofrontal cortex. J. Neurosci. 34, 953–962.

Driscoll, I., Hamilton, D.A., Petropoulos, H., Yeo, R.A., Brooks, W.M., Baumgartner, R.N., Sutherland, R.J., 2003. The aging hippocampus: cognitive, biochemical and structural findings. Cerebr. Cortex 13, 1344–1351.

Gould, R.W., Garg, P.K., Garg, S., Nader, M.A., 2013. Effects of nicotinic acetylcholine receptor agonists on cognition in rhesus monkeys with a chronic cocaine self-administration history. Neuropharmacology 64, 479–488.

Guzman-Mejia, F., Lopez-Rubalcava, C., Gonzalez-Espinosa, C., 2018. Stimulation of nAchRalpha7 receptor inhibits TNF synthesis and secretion in response to LPS treatment of mast cells by targeting ERK1/2 and TACE activation. J. Neuroimmune Pharmacol. 13, 39–52.

Hoeijmakers, J.H., 2009. DNA damage, aging, and cancer. N. Engl. J. Med. 361, 1475–1485.

Huang, C., Irwin, M.G., Wong, G.T.C., Chang, R.C.C., 2018. Evidence of the impact of systemic inflammation on neuroinflammation from a non-bacterial endotoxin animal model. J. Neuroinflammation 15, 147.

Iacovoni, J.S., Caron, P., Lassadi, I., Nicolas, E., Massip, L., Trouche, D., Legube, G., 2010. High-resolution profiling of gammaH2AX around DNA double strand breaks in the mammalian genome. EMBO J. 29, 1446–1457.

Ittner, L.M., Gotz, J., 2011. Amyloid-beta and tau–a toxic pas de deux in Alzheimer's disease. Nat. Rev. Neurosci. 12, 65–72.

Jackson, S.P., Bartek, J., 2009. The DNA-damage response in human biology and disease. Nature 461, 1071–1078.

Jayadev, S., Nesser, N.K., Hopkins, S., Myers, S.J., Case, A., Lee, R.J., Seaburg, L.A., Uo, T., Murphy, S.P., Morrison, R.S., Garden, G.A., 2011. Transcription factor p53 influences microglial activation phenotype. Glia 59, 1402–1413.

Kamer, A.R., Galoyan, S.M., Haile, M., Kline, R., Boutajangout, A., Li, Y.S., Bekker, A., 2012. Meloxicam improves object recognition memory and modulates glial activation after splenectomy in mice. Eur. J. Anaesthesiol. 29, 332–337.

Kim, S.Y., Choi, S.H., Rollema, H., Schwam, E.M., McRae, T., Dubrava, S., Jacobsen, J., 2014. Phase II crossover trial of varenicline in mild-to-moderate Alzheimer's disease. Dement. Geriatr. Cognit. Disord. 37, 232–245.

Kruk-Slomka, M., Budzynska, B., Biala, G., 2012. Involvement of cholinergic receptors in the different stages of memory measured in the modified elevated plus maze test in mice. Pharmacol. Rep. 64, 1066–1080.

Lane, D.P., Crawford, L.V., 1979. T antigen is bound to a host protein in SV40-transformed cells. Nature 278, 261–263.

Le Freche, H., Brouillette, J., Fernandez-Gomez, F.J., Patin, P., Caillierez, R., Zommer, N., Sergeant, N., Buee-Scherrer, V., Lebuffe, G., Blum, D., Buee, L., 2012. Tau phosphorylation and sevoflurane anesthesia: an association to postoperative cognitive impairment. Anesthesiology 116, 779–787.

Leger, M., Quiedeville, A., Bouet, V., Haelewyn, B., Boulouard, M., Schumann-Bard, P., Freret, T., 2013. Object recognition test in mice. Nat. Protoc. 8, 2531–2537.

Li, Y., Pan, K., Chen, L., Ning, J.L., Li, X., Yang, T., Terrando, N., Gu, J., Tao, G., 2016. Deferoxamine regulates neuroinflammation and iron homeostasis in a mouse model of postoperative cognitive dysfunction. J. Neuroinflammation 13, 268.

Mandelkow, E.M., Schweers, O., Drewes, G., Biernat, J., Gustke, N., Trinczek, B., Mandelkow, E., 1996. Structure, microtubule interactions, and phosphorylation of tau protein. Ann. N. Y. Acad. Sci. 777, 96–106.

Marks, M.J., O'Neill, H.C., Wynalda-Camozzi, K.M., Ortiz, N.C., Simmons, E.E., Short, C.A., Butt, C.M., McIntosh, J.M., Grady, S.R., 2015. Chronic treatment with varenicline changes expression of four nAChR binding sites in mice. Neuropharmacology 99, 142–155.

Mocking, R.J., Patrick Pflanz, C., Pringle, A., Parsons, E., McTavish, S.F., Cowen, P.J., Harmer, C.J., 2013. Effects of short-term varenicline administration on emotional and cognitive processing in healthy, non-smoking adults: a randomized, double-blind, study. Neuropsychopharmacology 38, 476–484.

Morris, M., Maeda, S., Vossel, K., Mucke, L., 2011. The many faces of tau. Neuron 70, 410–426.

Ng, D.C., Lin, B.H., Lim, C.P., Huang, G., Zhang, T., Poli, V., Cao, X., 2006. Stat3 regulates microtubules by antagonizing the depolymerization activity of stathmin. J. Cell Biol. 172, 245–257.

Nicolas, C.S., Peineau, S., Amici, M., Csaba, Z., Fafouri, A., Javalet, C., Collett, V.J., Hildebrandt, L., Seaton, G., Choi, S.L., Sim, S.E., Bradley, C., Lee, K., Zhuo, M., Kaang, B.K., Gressens, P., Dournaud, P., Fitzjohn, S.M., Bortolotto, Z.A., Cho, K., Collingridge, G.L., 2012. The Jak/STAT pathway is involved in synaptic plasticity. Neuron 73, 374–390.

Nilson, A.N., English, K.C., Gerson, J.E., Barton Whittle, T., Nicolas Crain, C., Xue, J., Sengupta, U., Castillo-Carranza, D.L., Zhang, W., Gupta, P., Kayed, R., 2017. Tau oligomers associate with inflammation in the brain and retina of tauopathy mice and in neurodegenerative diseases. J. Alzheimers Dis. 55, 1083–1099.

Park, S.J., Shin, E.J., Min, S.S., An, J., Li, Z., Hee Chung, Y., Hoon Jeong, J., Bach, J.H., Nah, S.Y., Kim, W.K., Jang, C.G., Kim, Y.S., Nabeshima, Y., Nabeshima, T., Kim, H.C., 2013. Inactivation of JAK2/STAT3 signaling axis and downregulation of M1 mAChR cause cognitive impairment in klotho mutant mice, a genetic model of aging. Neuropsychopharmacology 38, 1426–1437.

Picciotto, M.R., Brunzell, D.H., Caldarone, B.J., 2002. Effect of nicotine and nicotinic receptors on anxiety and depression. Neuroreport 13, 1097–1106.

Posadas, I., Lopez-Hernandez, B., Cena, V., 2013. Nicotinic receptors in neurodegeneration. Curr. Neuropharmacol. 11, 298–314.

Qiu, L.L., Ji, M.H., Zhang, H., Yang, J.J., Sun, X.R., Tang, H., Wang, J., Liu, W.X., Yang, J.J., 2016. NADPH oxidase 2-derived reactive oxygen species in the hippocampus might contribute to microglial activation in postoperative cognitive dysfunction in aged mice. Brain Behav. Immun. 51, 109–118.

Rosas-Ballina, M., Olofsson, P.S., Ochani, M., Valdes-Ferrer, S.I., Levine, Y.A., Reardon, C., Tusche, M.W., Pavlov, V.A., Andersson, U., Chavan, S., Mak, T.W., Tracey, K.J., 2011. Acetylcholine-synthesizing T cells relay neural signals in a vagus nerve circuit. Science 334, 98–101.

Schuitemaker, A., Dik, M.G., Veerhuis, R., Scheltens, P., Schoonenboom, N.S., Hack, C.E., Blankenstein, M.A., Jonker, C., 2009. Inflammatory markers in AD and MCI patients with different biomarker profiles. Neurobiol. Aging 30, 1885–1889.

Schwarz, N., Kastaun, S., Schoenburg, M., Kaps, M., Gerriets, T., 2013. Subjective impairment after cardiac surgeries: the relevance of postoperative cognitive decline in daily living. Eur. J. Cardio. Thorac. Surg. 43, e162–166.

Shiotsuki, H., Yoshimi, K., Shimo, Y., Funayama, M., Takamatsu, Y., Ikeda, K., Takahashi, R., Kitazawa, S., Hattori, N., 2010. A rotarod test for evaluation of motor skill learning. J. Neurosci. Methods 189, 180–185.

Silbert, B.S., Evered, L.A., Scott, D.A., 2014. Incidence of postoperative cognitive dysfunction after general or spinal anaesthesia for extracorporeal shock wave lithotripsy. Br. J. Anaesth. 113, 784–791.

Steinmetz, J., Siersma, V., Kessing, L.V., Rasmussen, L.S., Group, I., 2013. Is postoperative cognitive dysfunction a risk factor for dementia? A cohort follow-up study. Br. J. Anaesth. 110 (Suppl. 1), i92–97.

Terrando, N., Yang, T., Ryu, J.K., Newton, P.T., Monaco, C., Feldmann, M., Ma, D., Akassoglou, K., Maze, M., 2015. Stimulation of the alpha7 nicotinic acetylcholine receptor protects against neuroinflammation after tibia fracture and endotoxemia in mice. Mol. Med. 20, 667–675.

Tolnay, M., Probst, A., 1999. REVIEW: tau protein pathology in Alzheimer's disease and related disorders. Neuropathol. Appl. Neurobiol. 25, 171–187.

Tovote, P., Fadok, J.P., Luthi, A., 2015. Neuronal circuits for fear and anxiety. Nat. Rev. Neurosci. 16, 317–331.

Tuman, K.J., McCarthy, R.J., Najafi, H., Ivankovich, A.D., 1992. Differential effects of advanced age on neurologic and cardiac risks of coronary artery operations. J. Thorac. Cardiovasc. Surg. 104, 1510–1517.

Tyagi, E., Agrawal, R., Nath, C., Shukla, R., 2010. Cholinergic protection via alpha7 nicotinic acetylcholine receptors and PI3K-Akt pathway in LPS-induced neuroinflammation. Neurochem. Int. 56, 135–142.

Vogelstein, B., Lane, D., Levine, A.J., 2000. Surfing the p53 network. Nature 408, 307–310.

Wan, Y., Xu, J., Ma, D., Zeng, Y., Cibelli, M., Maze, M., 2007. Postoperative impairment of cognitive function in rats: a possible role for cytokine-mediated inflammation in the hippocampus. Anesthesiology 106, 436–443.

Wan, Y., Xu, J., Meng, F., Bao, Y., Ge, Y., Lobo, N., Vizcaychipi, M.P., Zhang, D., Gentleman, S.M., Maze, M., Ma, D., 2010. Cognitive decline following major surgery is associated with gliosis, beta-amyloid accumulation, and tau phosphorylation in old mice. Crit. Care Med. 38, 2190–2198.

Wang, J.Z., Liu, F., 2008. Microtubule-associated protein tau in development, degeneration and protection of neurons. Prog. Neurobiol. 85, 148–175.